Improved efficiency of high resolution thermal and cold neutron imaging

A.S. Tremsin[1], J.B. McPhate[1], J.V. Vallerga[1], O.H.W. Siegmund[1], W.B. Feller[2] , E. Lehmann[3] , M. Dawson[4]

[1]*University of California at Berkeley, CA 94720, USA*

[2]*Nova Scientific, Inc, Sturbridge, MA 01566, USA*

[3]*Paul Scherrer Institute, Switzerland*

[4]*Helmholtz-Zentrum Berlin für Materialien und Energie GmbH*

Outline

- Neutron counting with microchannel plates
- Spatial and temporal resolution of neutron imaging with MCP detectors
- Applications:
  - *Energy resolved neutron radiography*
  - *Spatially resolved strain analysis*
  - *Material composition analysis*
  - *Imaging of dynamic magnetic fields*

Image FUV satellite

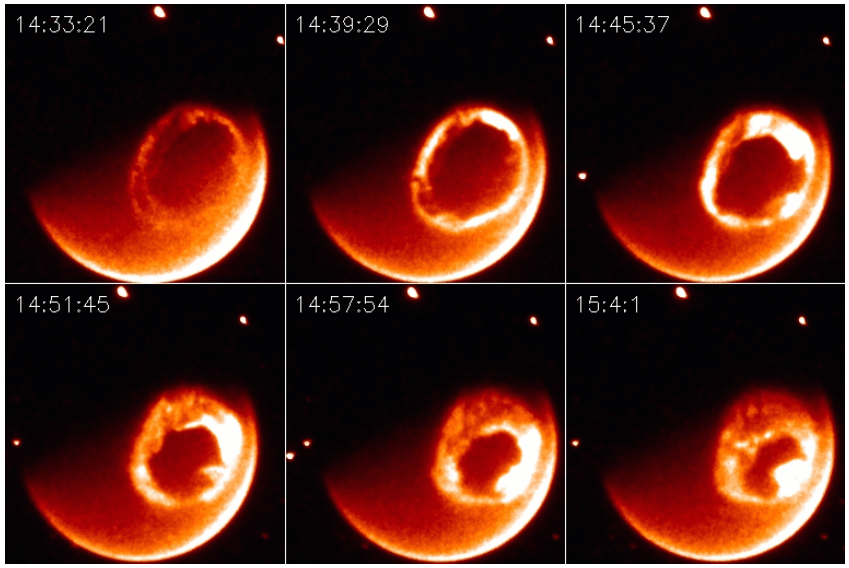

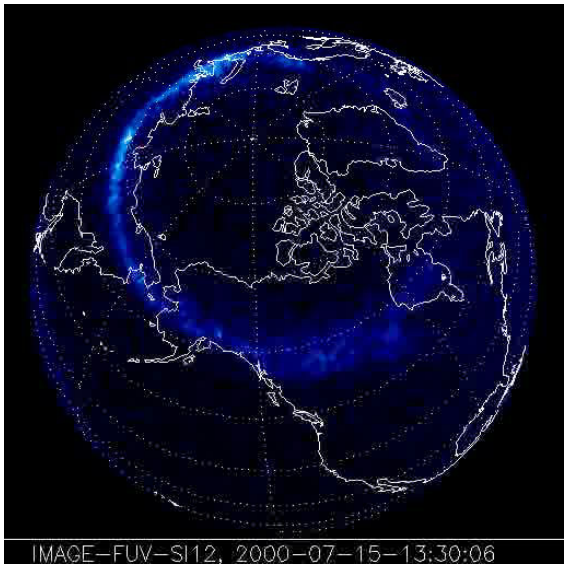

MCP electron amplifier

Circular-pore MCP

Single pore

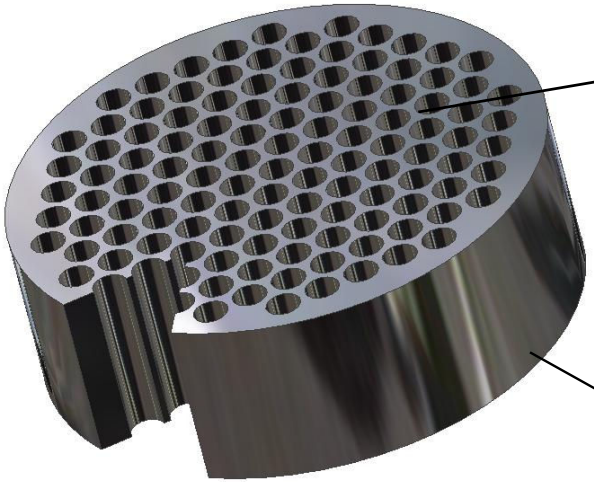

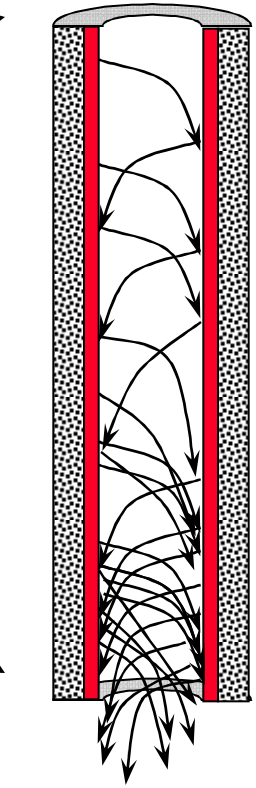

MCP detector configuration

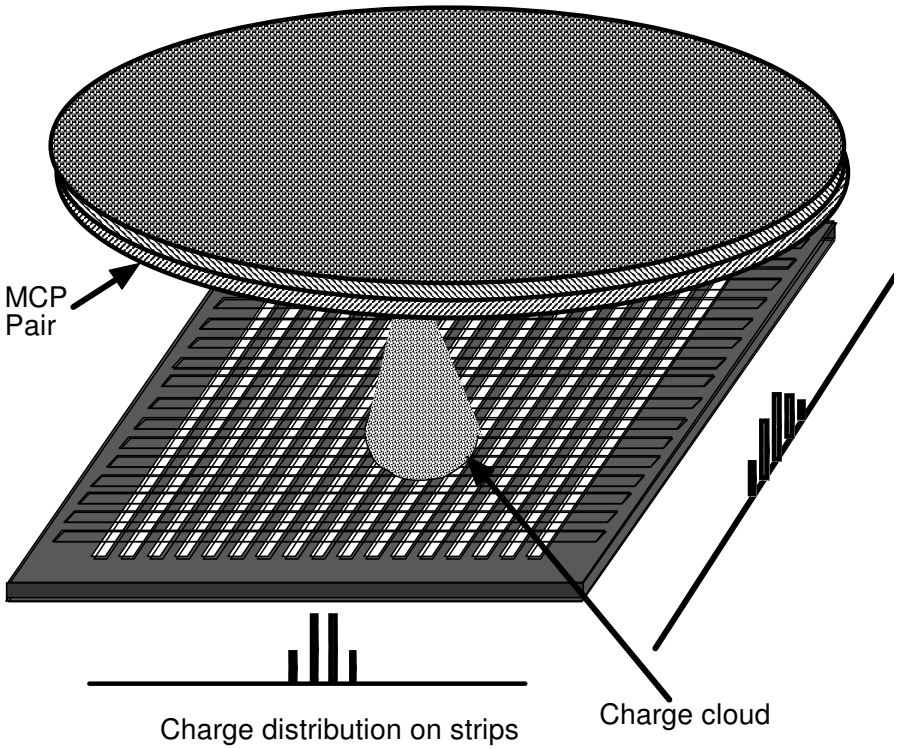

Schematic of an MCP detector

- Photon/e/ion/neutral particle and neutron counting
- XY coordinates and Time for each registered event
- Virtually no dark current /readout noise!

Principle of neutron detection with MCPs

Ranges of ^{4}He and ^{7}Li particles in MCP glass are 3.5 and 2 μm

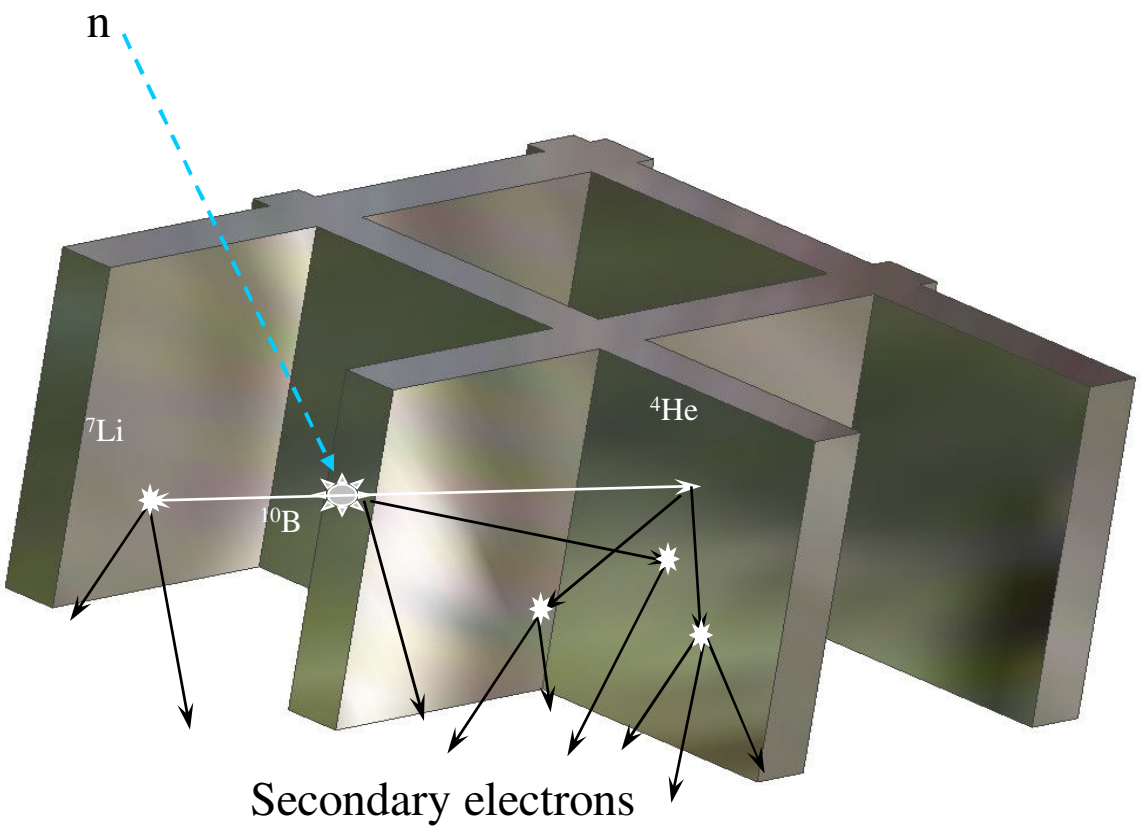

Detector hardware implementations

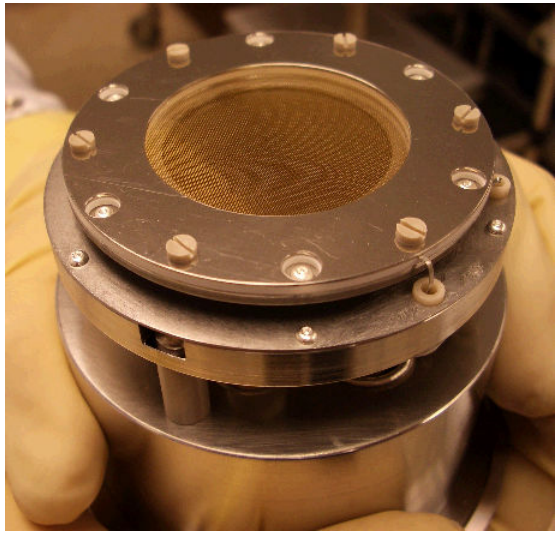

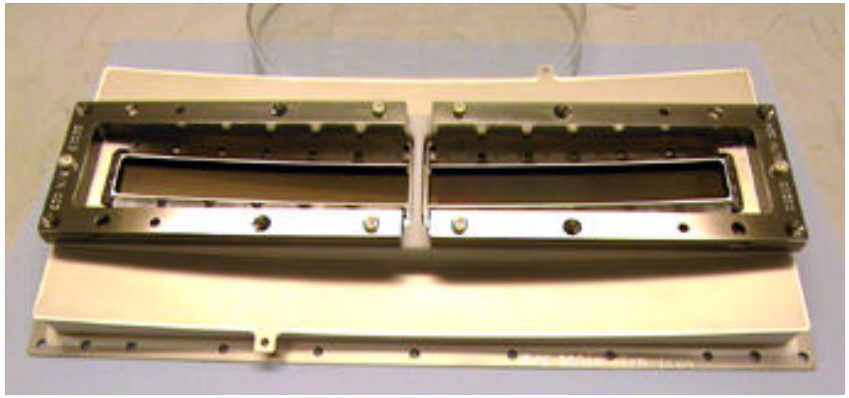

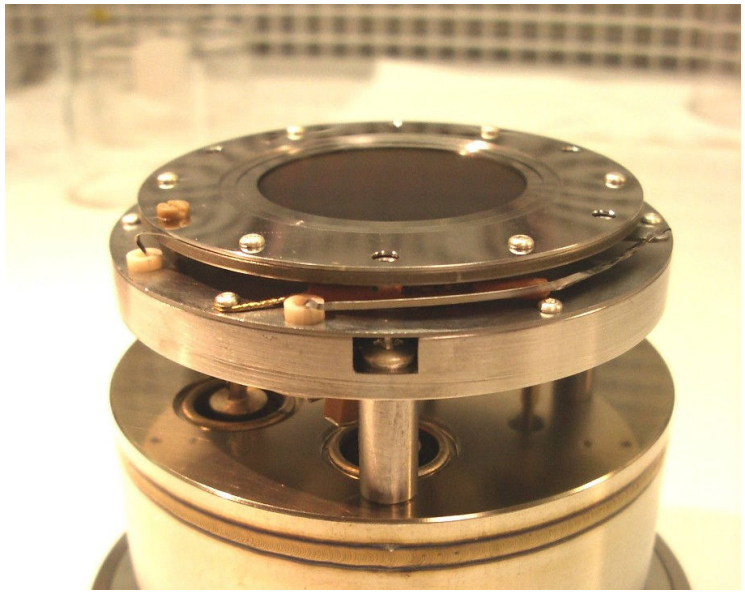

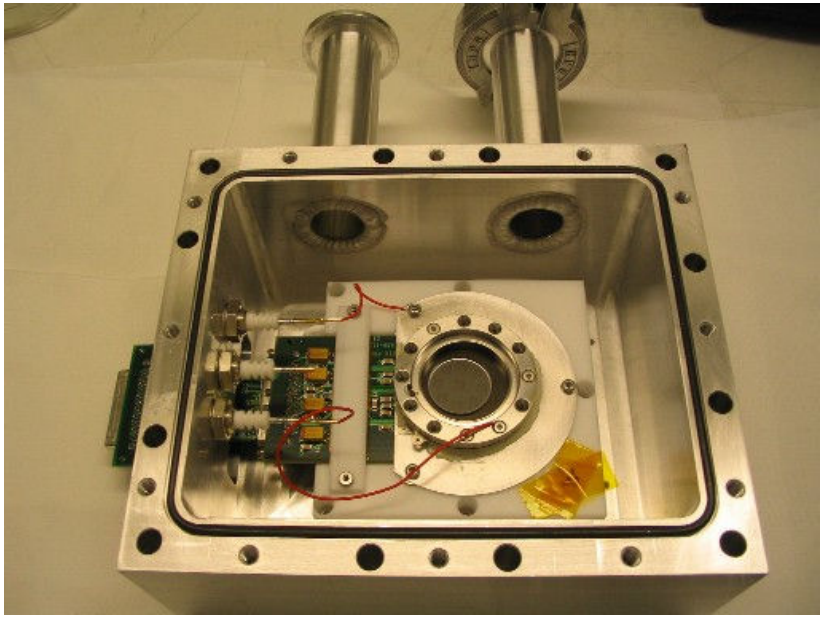

MCP detector with Medipix/Timepix readout

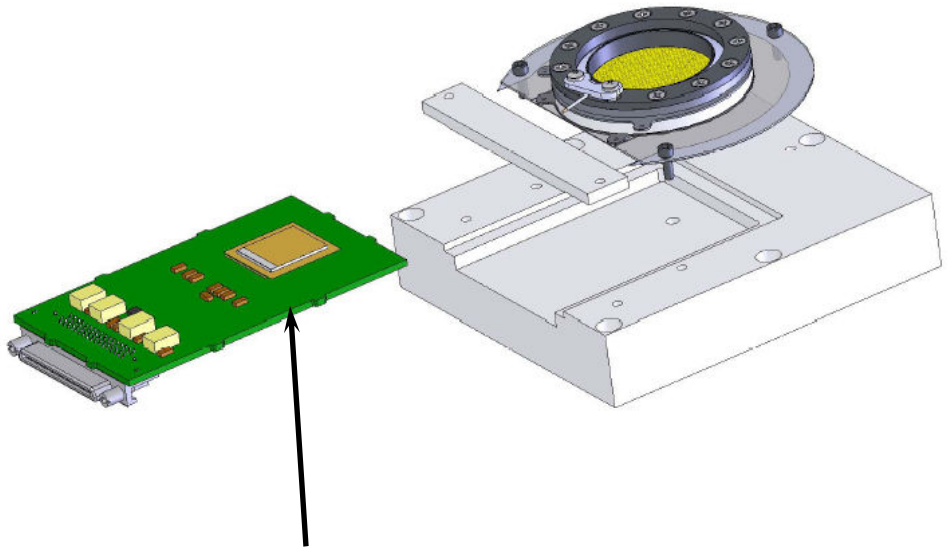

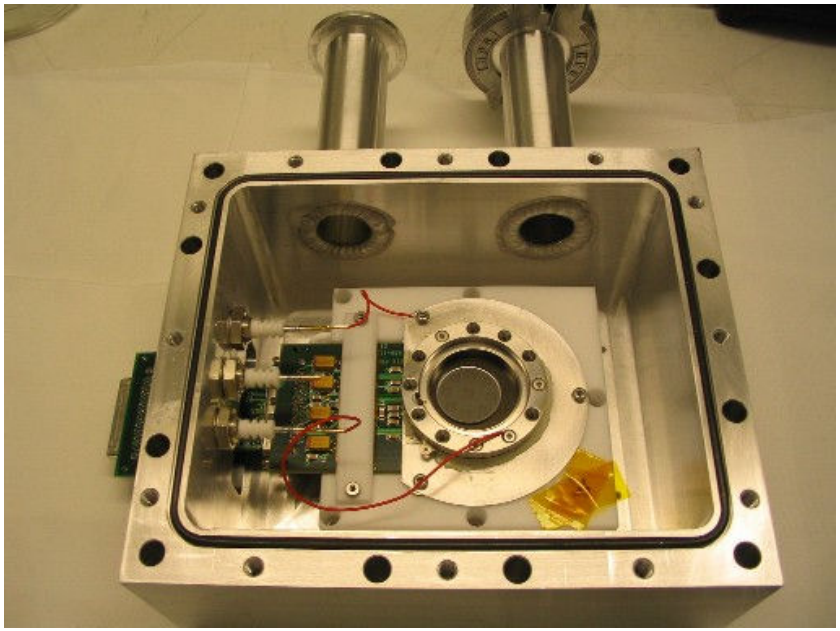

- 256 x 256 array of 55 µm pixels
- 100 kHz/pxl
- Frame rate: 1 kHz
- Low noise (<100e$^-$) = low gain operation (10 ke$^-$)
- ~1 W watt/chip, abuttable
- Developed at CERN

Stack of MCPs is placed 0.5-0.7 mm above Medipix2/TimePix readout

Muros readout electronics (NIKHEF) and PixelMan software (IEAP, CTU Prague) with Labview and C++ plugins (UCB)

Neutron detection efficiency

$$P_{detection} = P_1 * P_2 * P_3$$

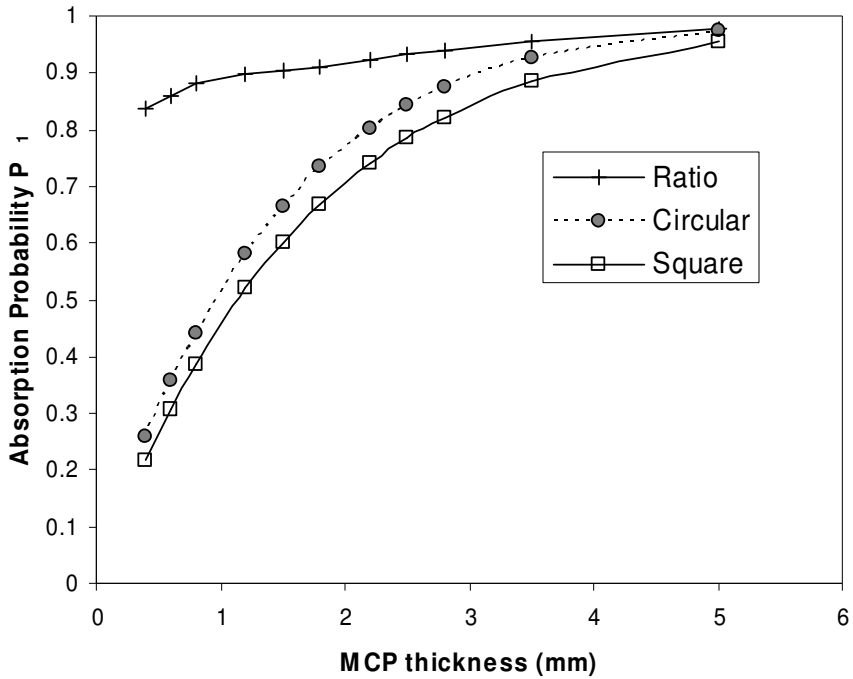

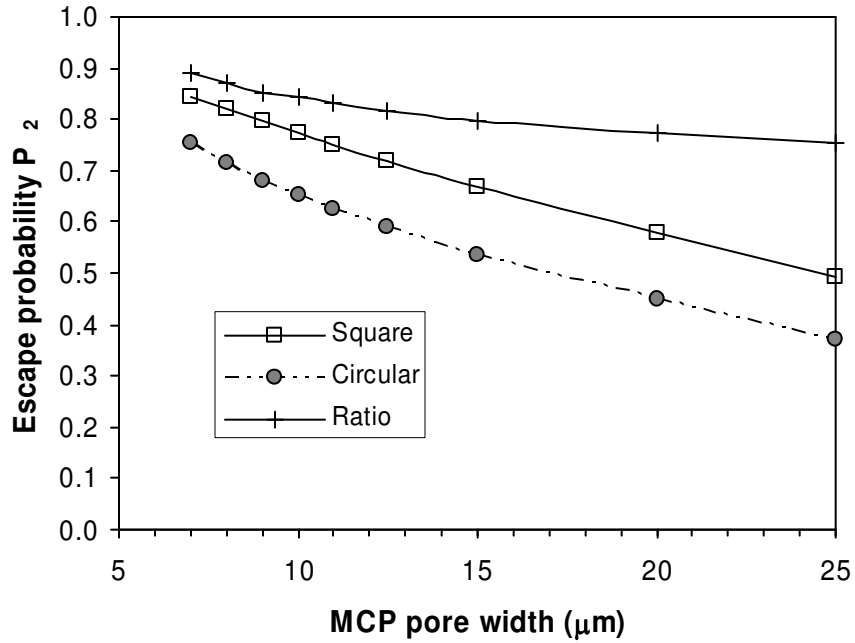

10 μm pores on 12 μm centers; $^{10}B_2O_3$ doping

$P_{detection}$ can exceed 50% for thermal neutrons

A.S. Tremsin, et al., Nucl. Instrum. Meth. A 539/1-2, pp. 278-311 (2005)

Escape probability P_2

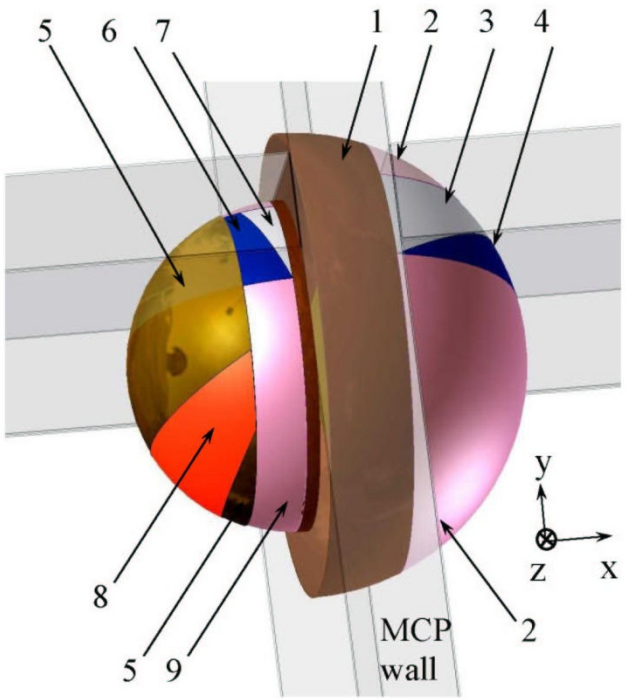

^{4}He escape semi-sphere

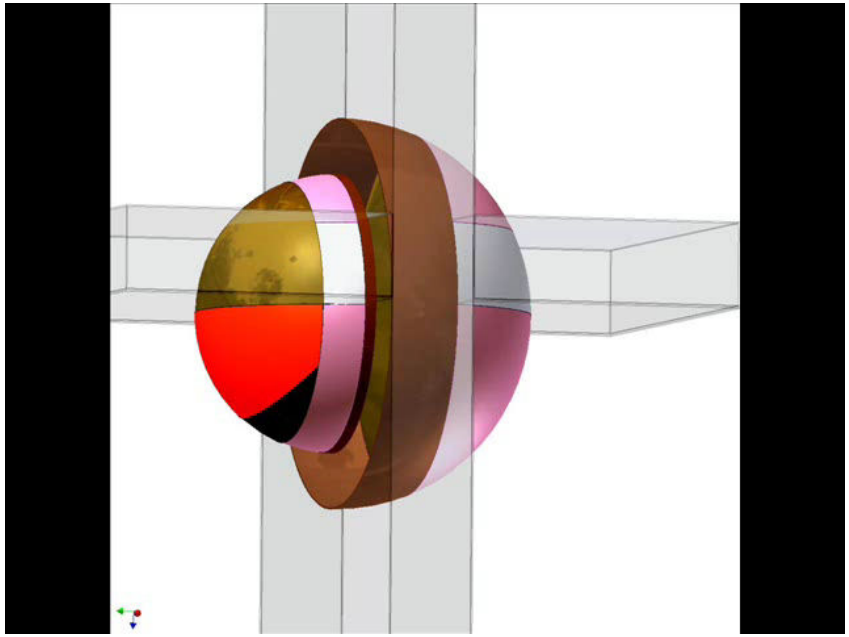

^{7}Li escape semi-sphere

^{4}He and ^{7}Li escape movie

Escape probability P_2

8 μm pores, 2 μm walls, square/circular pores

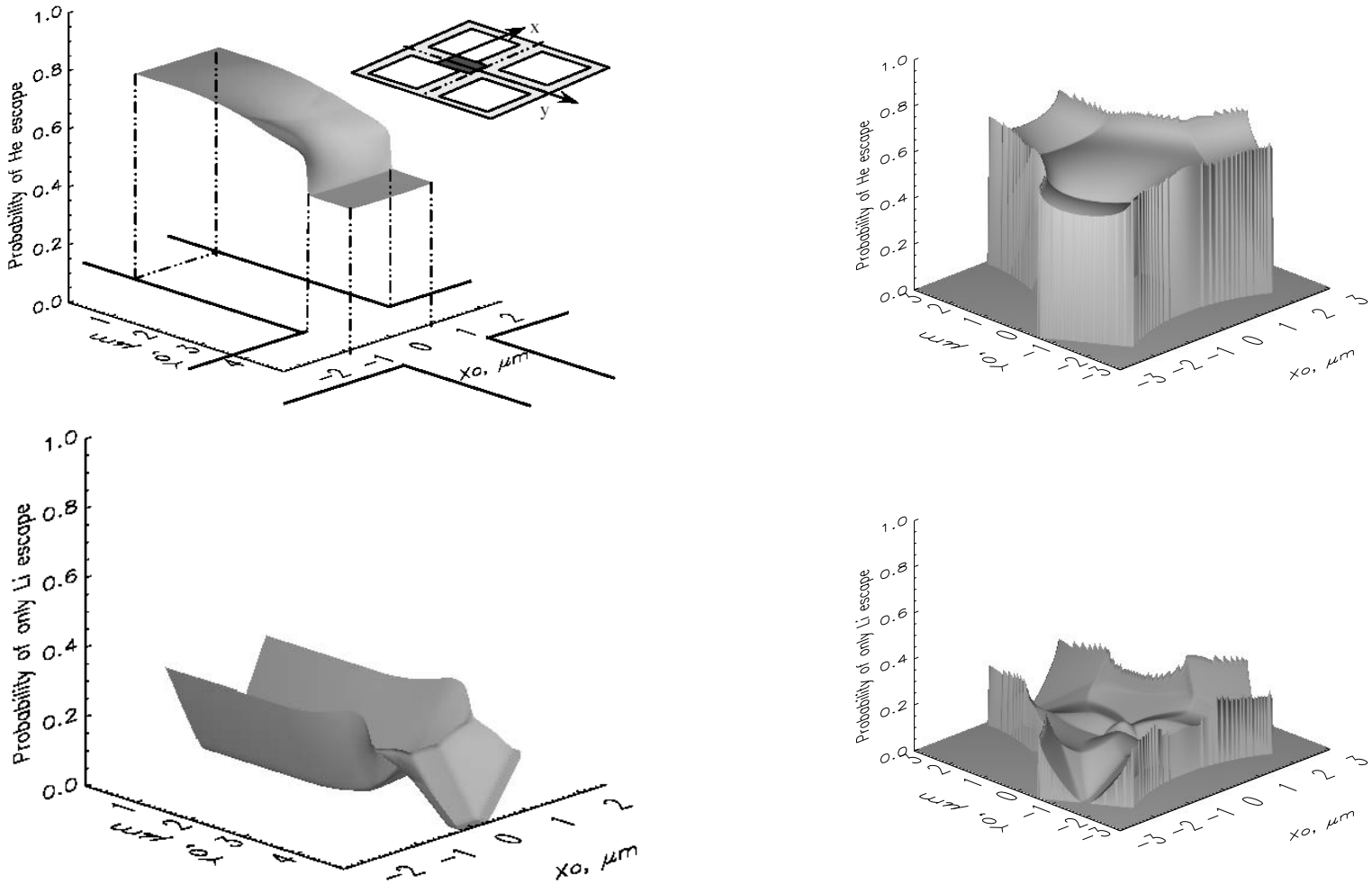

Neutron detection efficiency: measurement

Single frame **30 μs**: (ICON, PSI)
individual neutron events

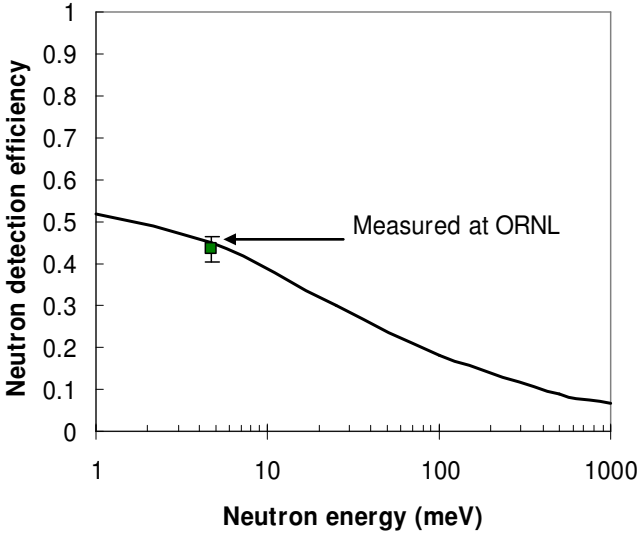

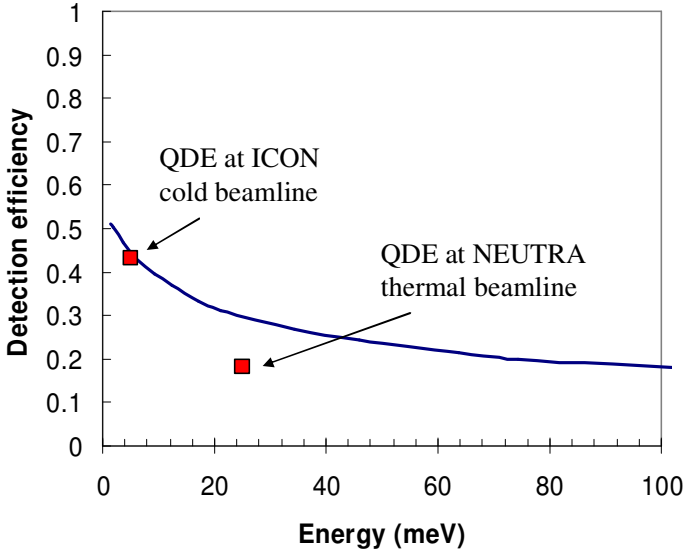

Measured data agrees with predictions

A. S. Tremsin, et al., Proc. SPIE 6945-41, (2008).
A.S. Tremsin, et al., Nucl. Instr. Meth. A 604 (2009) 140.

Neutron detection efficiency: previous results

Beam spectra:
ICON and NEUTRA, PSI

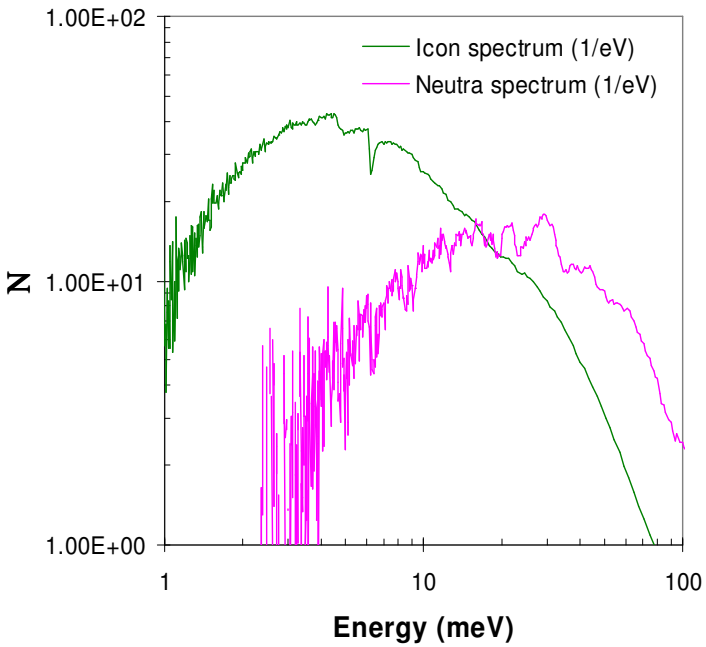

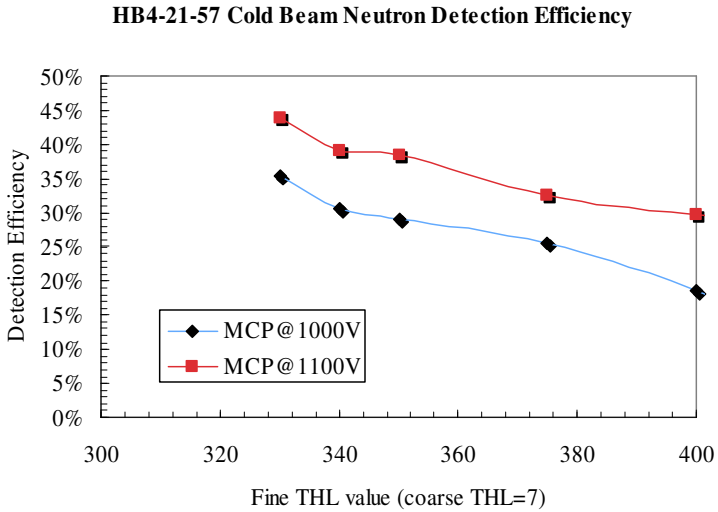

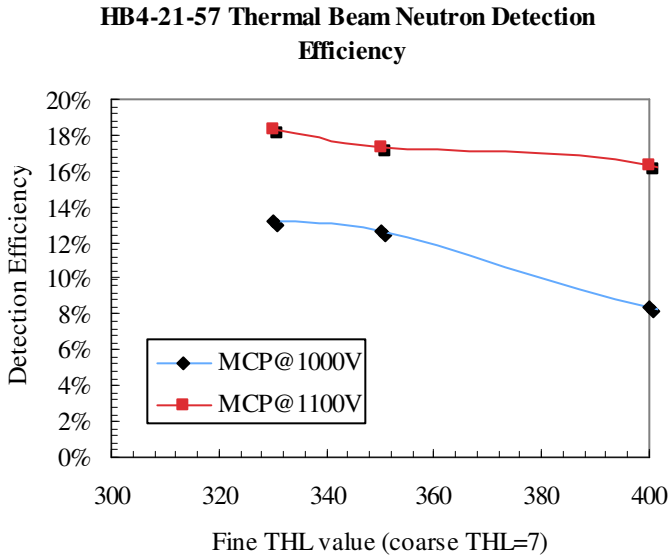

Neutron detection efficiency: ICON bamline

Single frame **30 μs**: (ICON, PSI)
individual neutron events

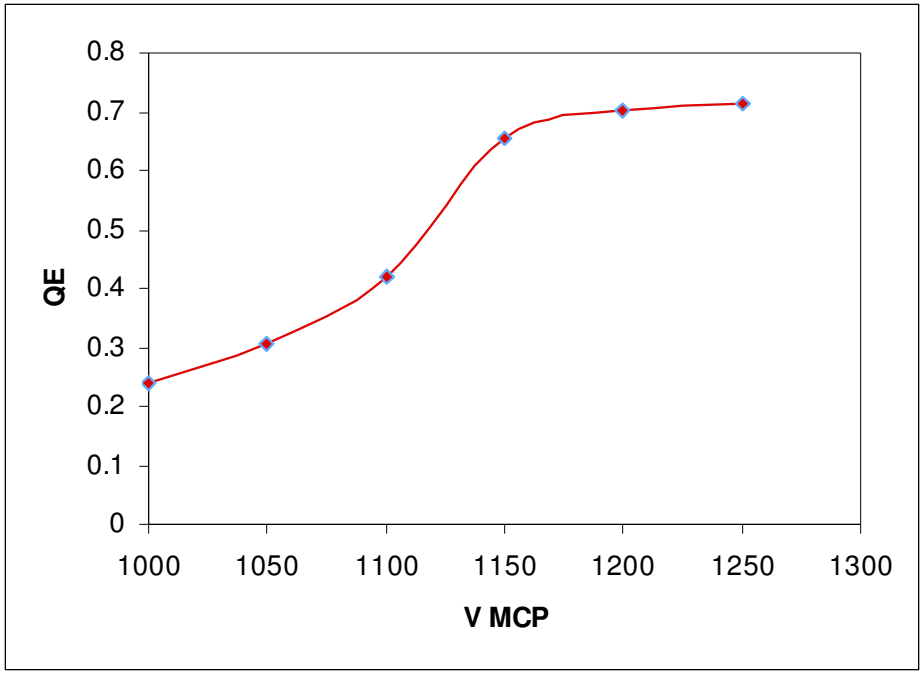

Measured data agrees with predictions

Neutron attenuation coefficient

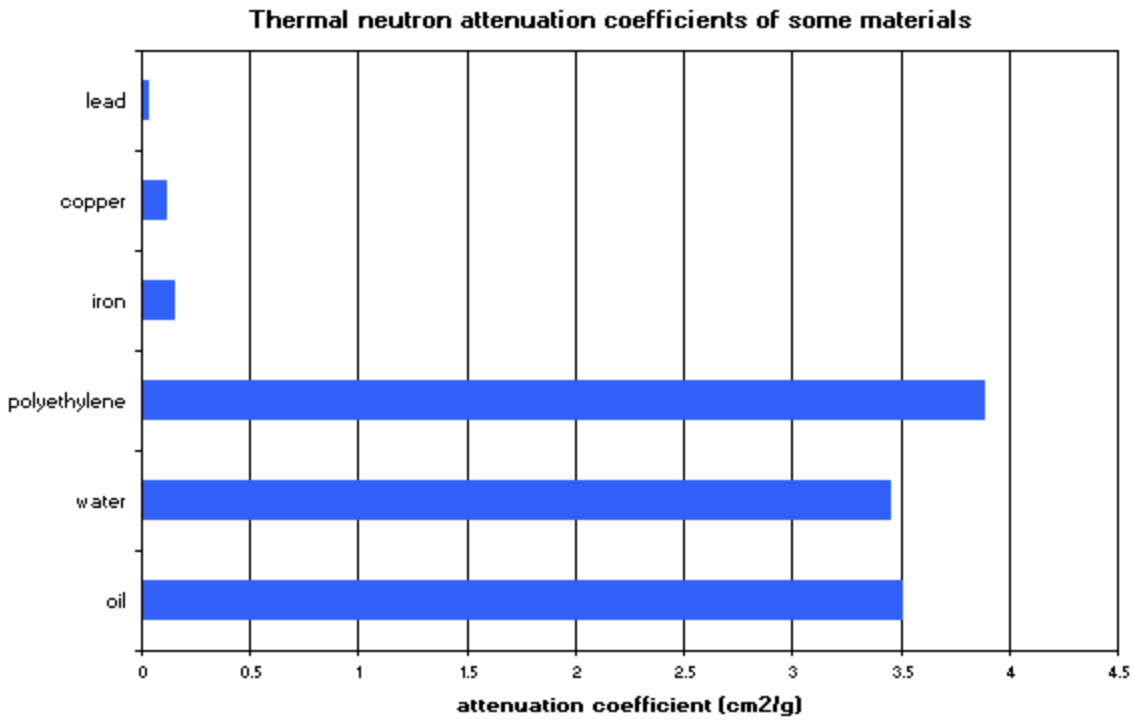

Source: Paul Scherrer Institute website

Applications: conventional neutron radiography

~7 mm

~7 mm

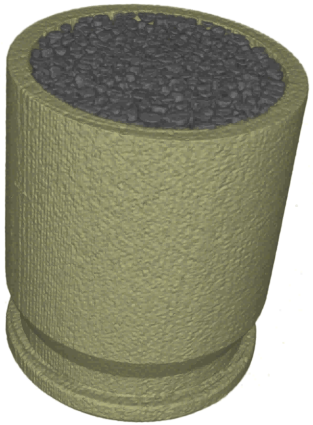

ICON cold neutron beamline.

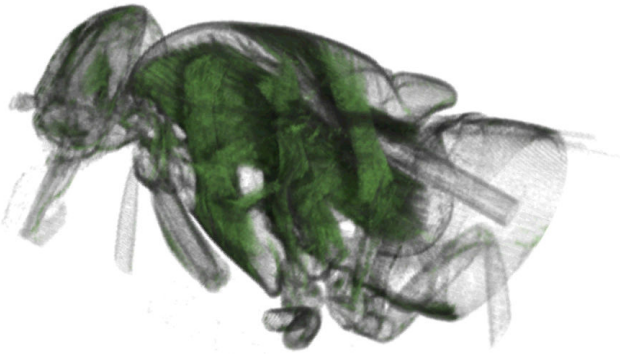

Reconstruction by Martin Dawson, HZB Berlin

Oil propagation inside of a fuel injector

14 mm

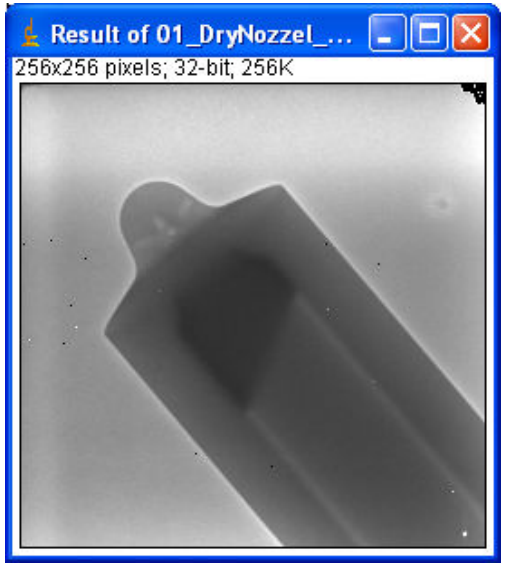

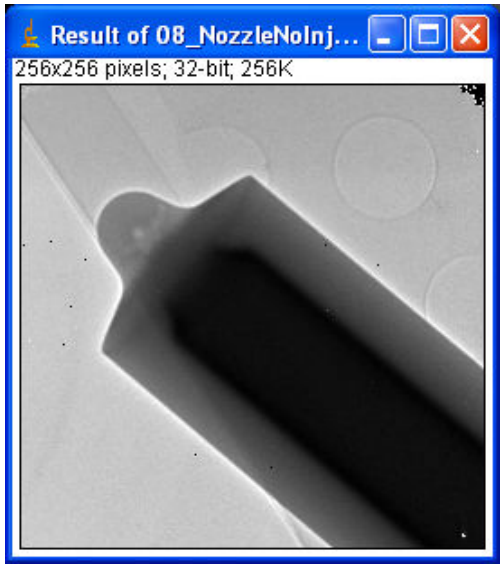

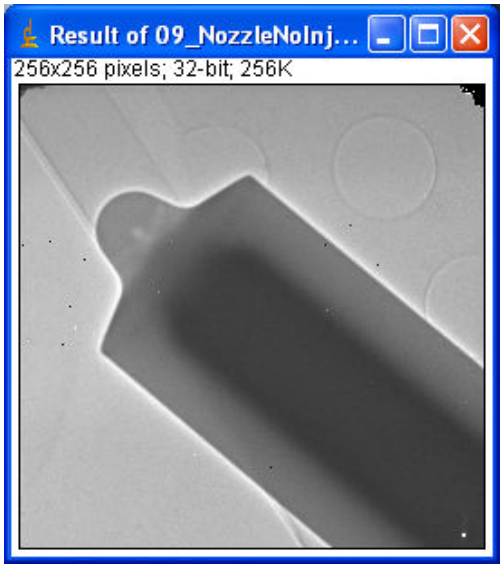

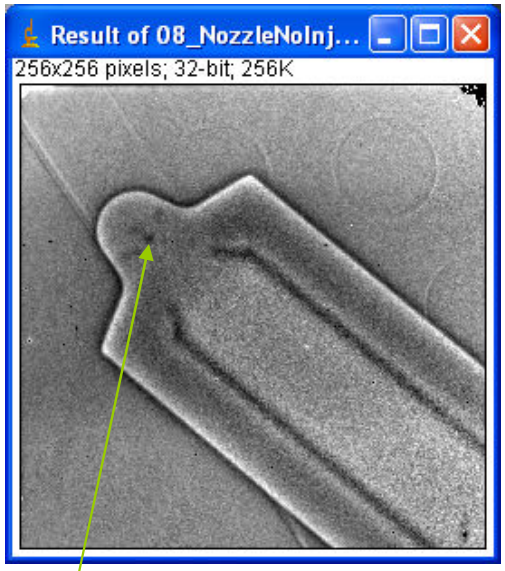

~100-200 μm injection holes

FRM2 reactor, ANTARES beamline,
In collaboration with ANTARES team
January 2009.

A.S. Tremsin, et al., IEEE NSS 2009, subm. IEEE Trans. Nucl. Sci.

Spatially resolved strain analysis

Time of flight and XY position is measured for every neutron

Pulsed source: 50 Hz

L/D ~100:1

Flight path 50 m

Flux ~10^6 n/cm^2/s (0.5-6 Å)

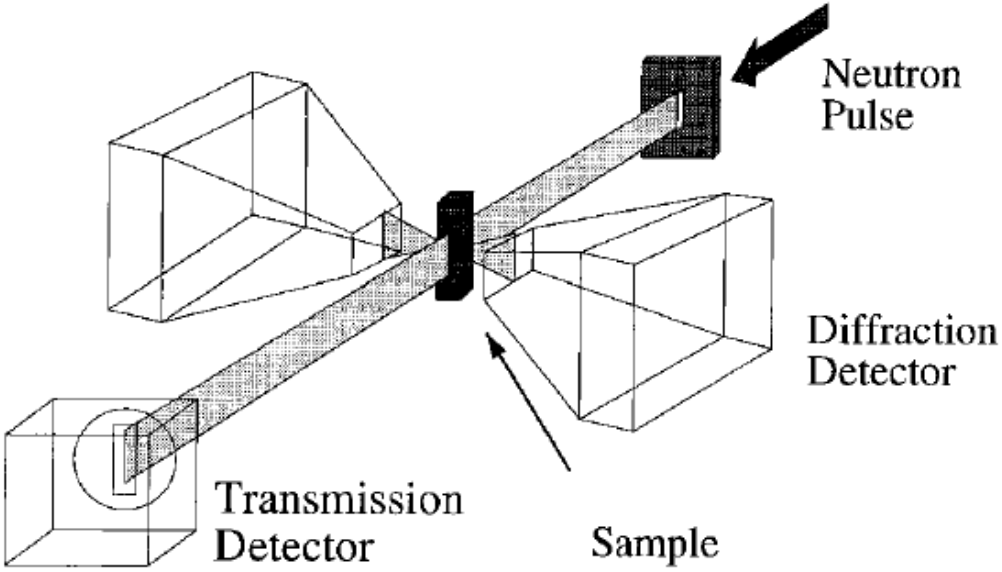

A. Steuwer, P.J. Withers, J.R. Santisteban et al., Phys. Stat. Sol. (a) 185, 221–230 (2001)

Coherent scattering – Bragg edges

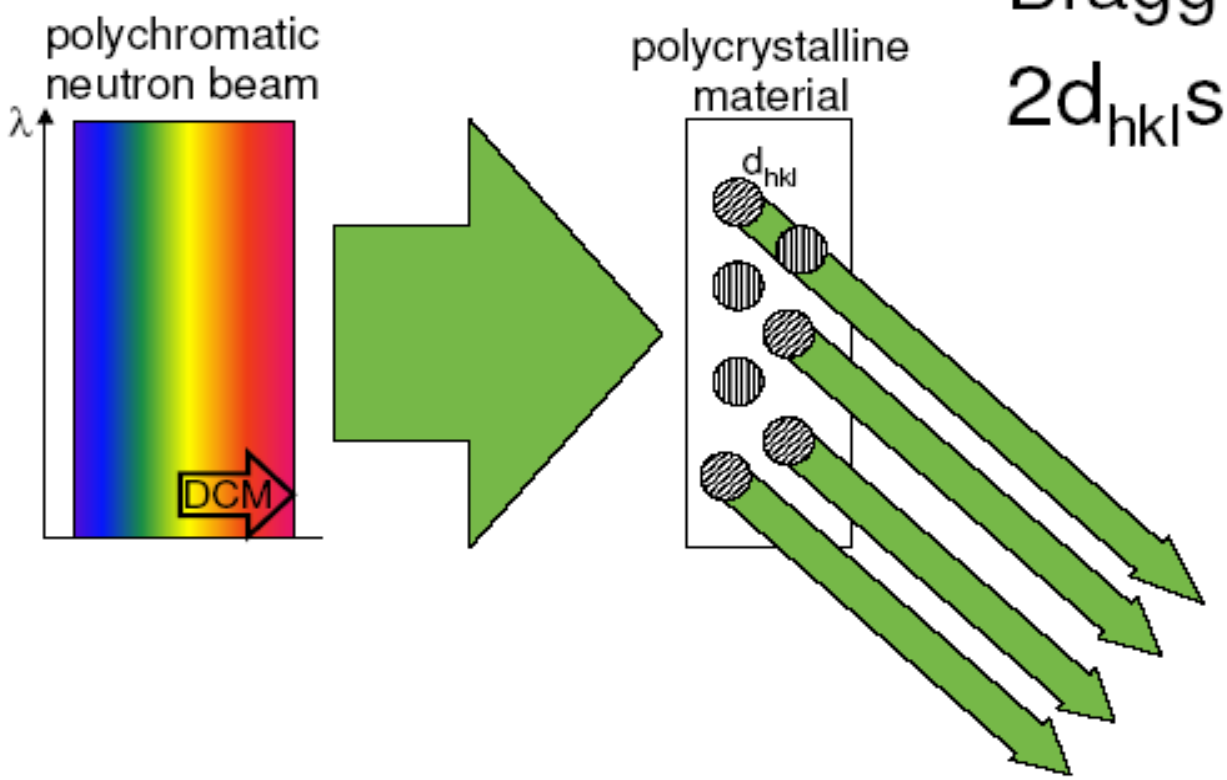

Bragg's law

$$2d_{hkl}\sin\theta=\lambda$$

Coherent scattering – Bragg edges

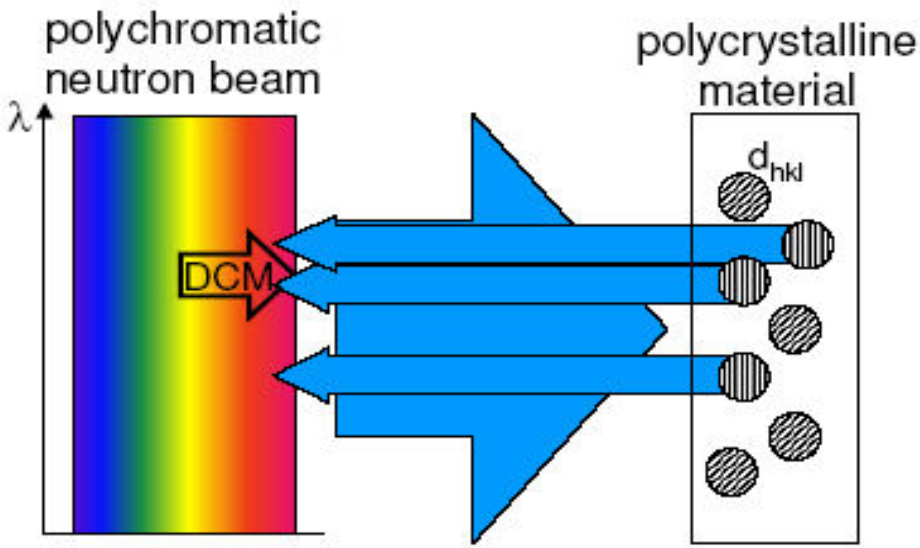

Bragg's law

$$2d_{hkl}\sin 90° = \lambda$$

Cross-sections of iron per atom

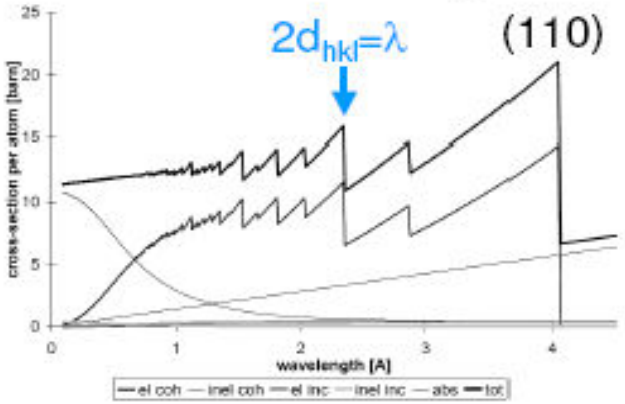

N. Kardjilov, HZB, Berlin

Cantilever sample: BCC steel (June 2009)

The cantilever is bent by 1 mm at the tip

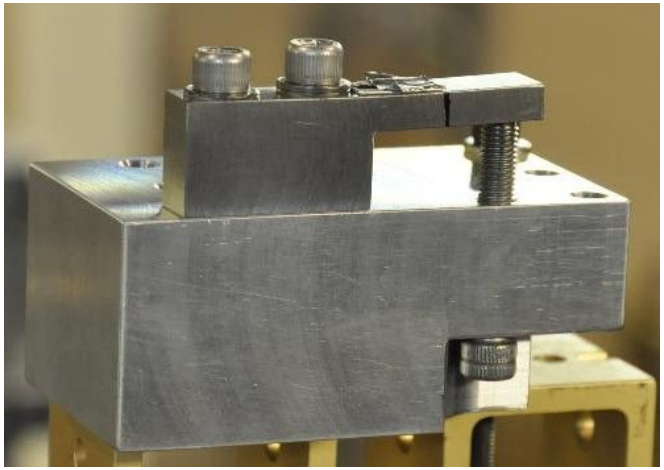

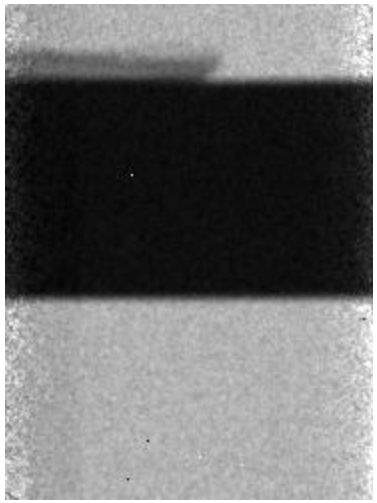

Full spectrum transmission image: 200s integration

Largest load on the cantilever: bent by 2 mm at the tip

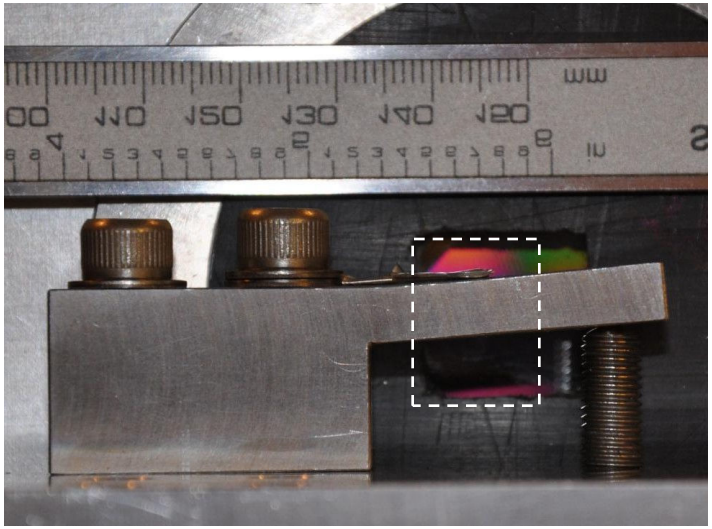

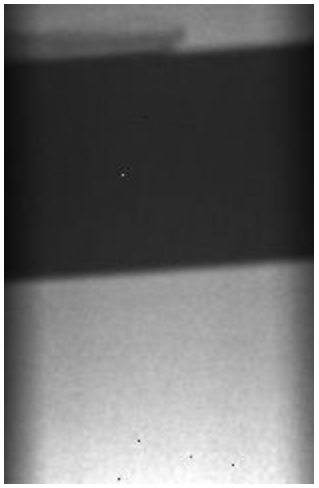

Largest load on the cantilever: bent by 2 mm at the tip

Residual bend, left after the 2mm load.

Cantilever sample: BCC steel

- T (~1 μs) relative to source trigger and position (~55 μm) for every neutron
- Neutron energy obtained from time of flight
- Transmission spectra within given area is calculated
- Limited statistics per 55x55 μm^2 pixel around 211 Bragg edge - need to integrate data from several pixels

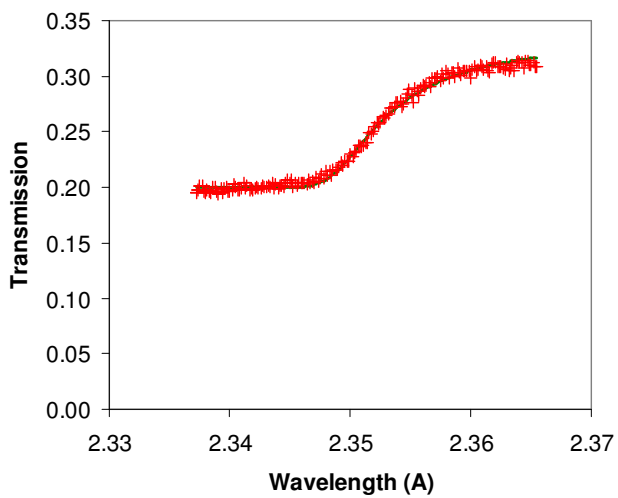

$$T(\lambda)\Big|_{\lambda_0,\sigma,\tau,C_1,C_2} = C_1 + C_2\left[erfc\left(\frac{\lambda_0-\lambda}{\sqrt{2}\sigma}\right) - \exp\left(\frac{\lambda_0-\lambda}{\tau}+\frac{\sigma^2}{2\tau^2}\right) * erfc\left(\frac{\lambda_0-\lambda}{\sqrt{2}\sigma}+\frac{\sigma}{\sqrt{2}\tau}\right)\right]$$

$$\frac{d(x,y)-d_0}{d_0} = \frac{\lambda(x,y)-\lambda_0}{\lambda_0}$$

Do the fit for every pixel – 65536 fits of coefficients

Cantilever sample: measured strain maps

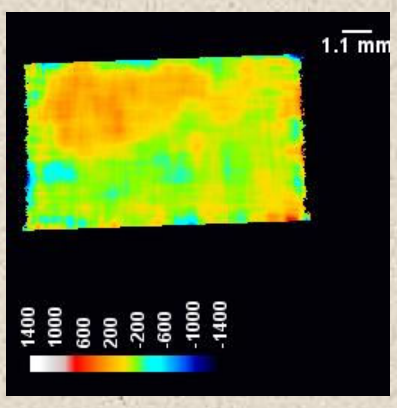

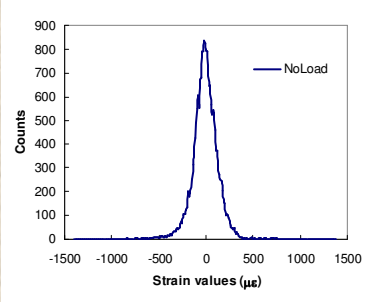

No load

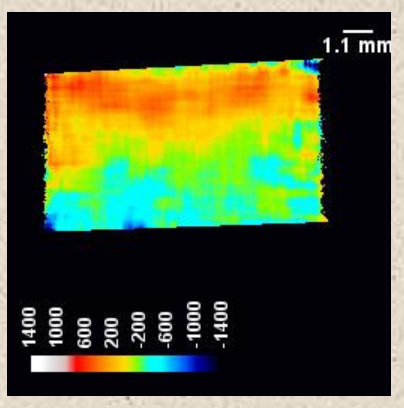

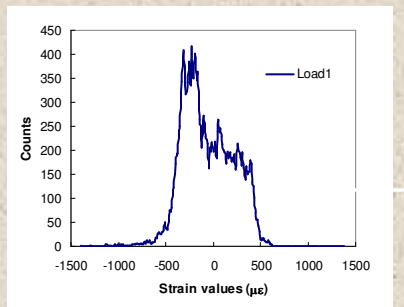

Bent by 0.5 mm

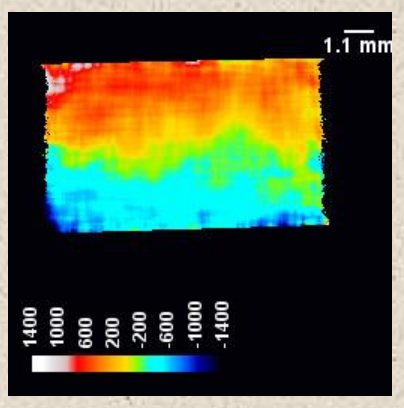

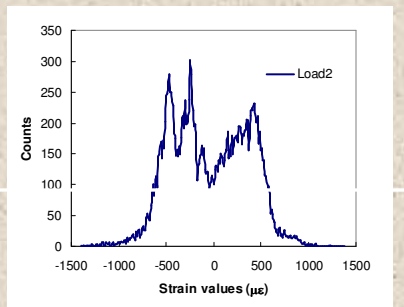

Bent by 1 mm

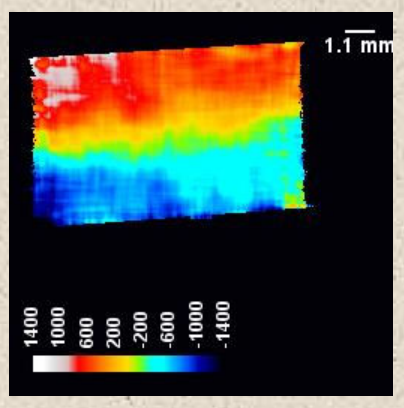

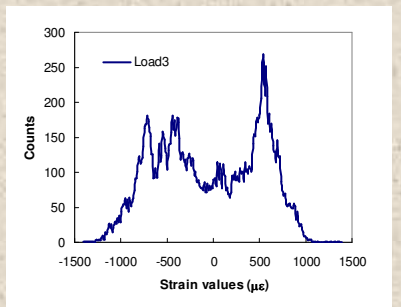

Bent by 2 mm

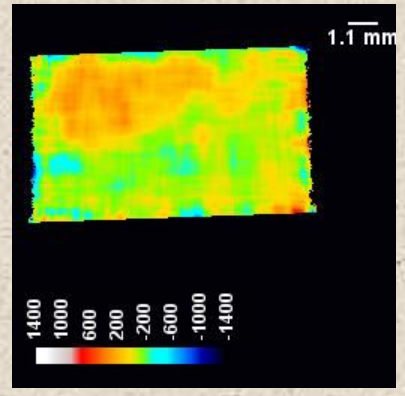

Residual

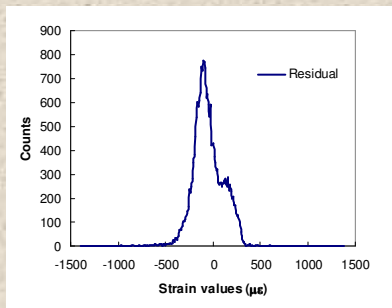

A. S. Tremsin, J. B. McPhate, A. Steuwer, W. Kockelmann, A. Paradowska, J. Kelleher, J. V. Vallerga, O. H. W. Siegmund, W. B. Feller, in preparation

Crack in FCC steel (June 2009)

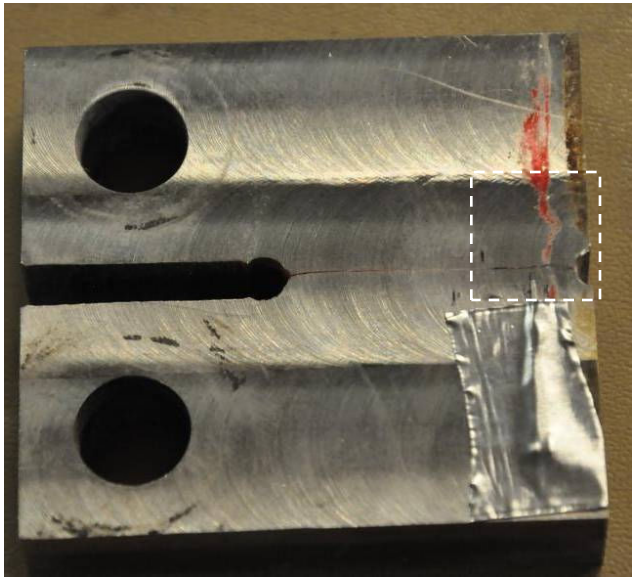

Strain map of area shown on the photos by a box

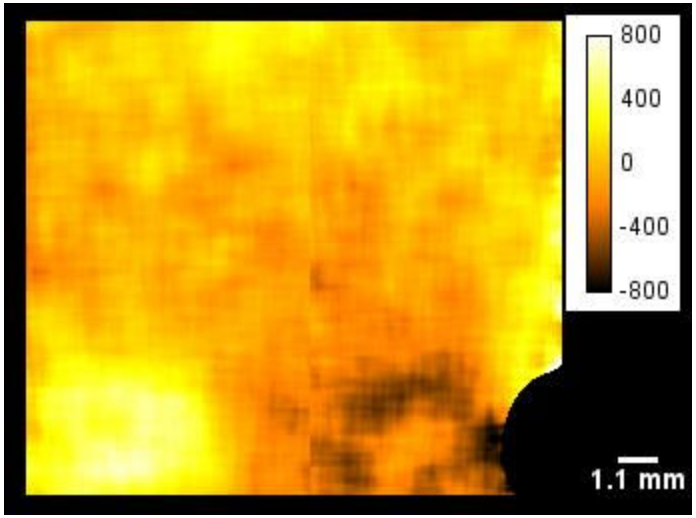

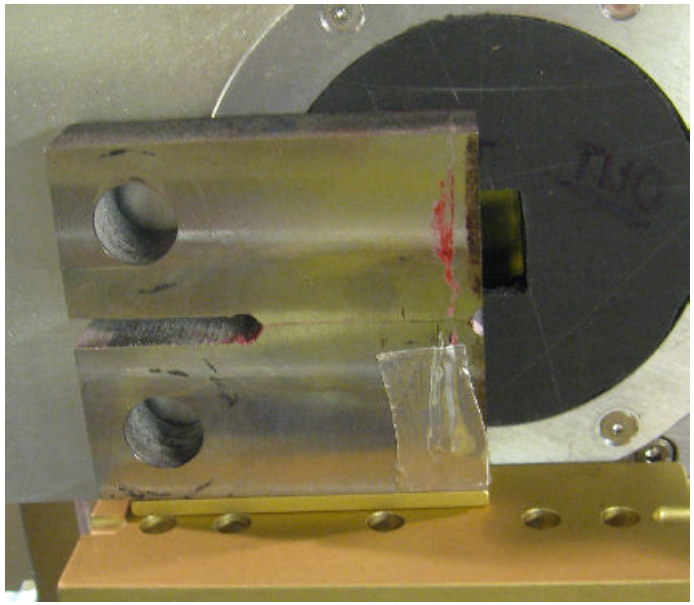

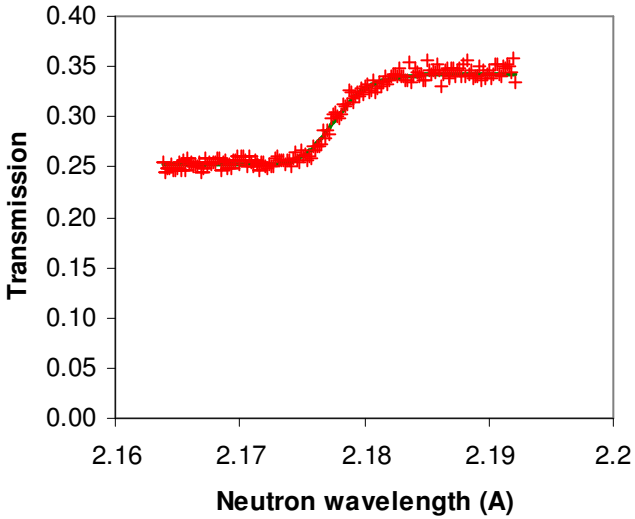

Magnetic field imaging through neutron spin interaction

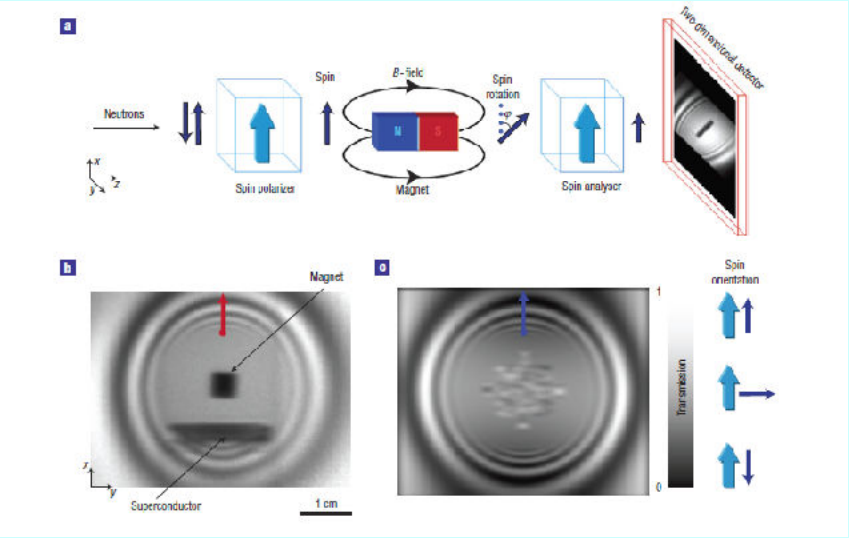

N. Kardjilov et al., Nature Phys. 4 (2008) 399–403

8 μs time slices stacked into a movie

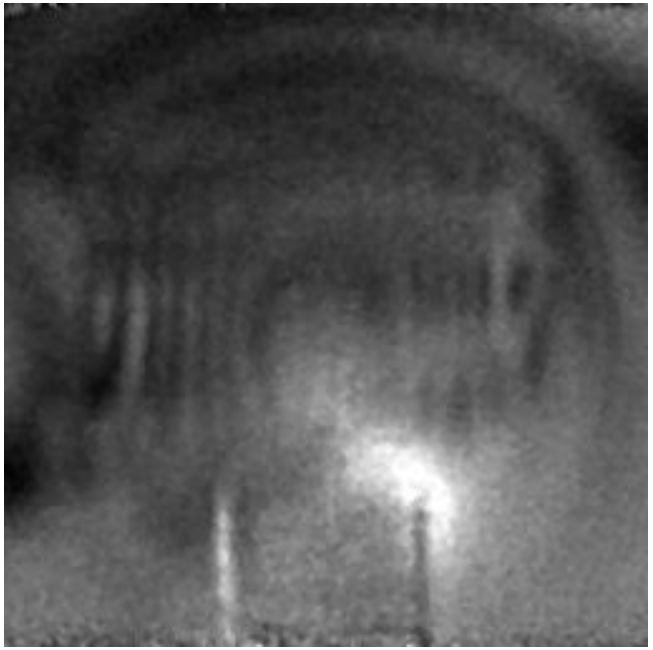

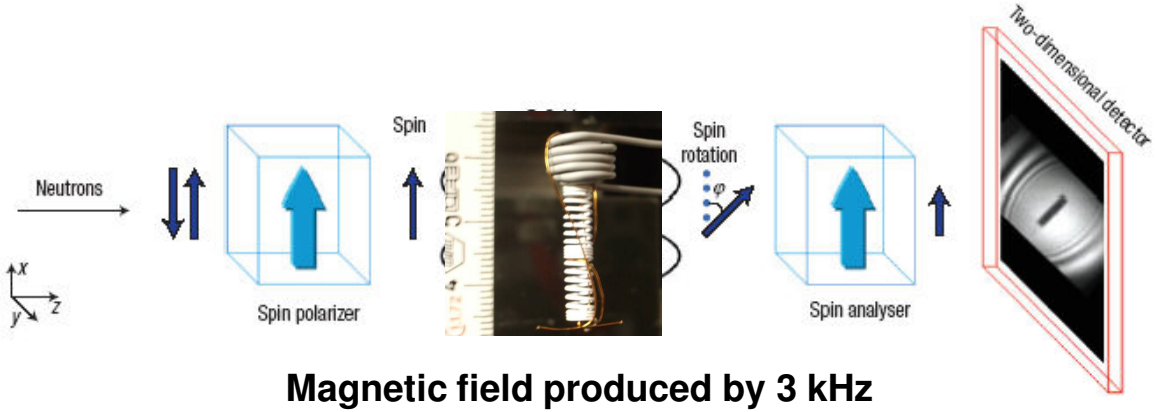

Magnetic field produced by 3 kHz AC current in a coil imaged

A. S. Tremsin, M. Dawson, N. Kardjilov, M. Strobl, I. Manke, J. B. McPhate, J. V. Vallerga, O. H. W. Siegmund, W. B. Feller, in preparation

Magnetic field imaging through neutron spin interaction

Magnetic field produced by 3 kHz AC current in a coil

8 μs time slices stacked into a movie

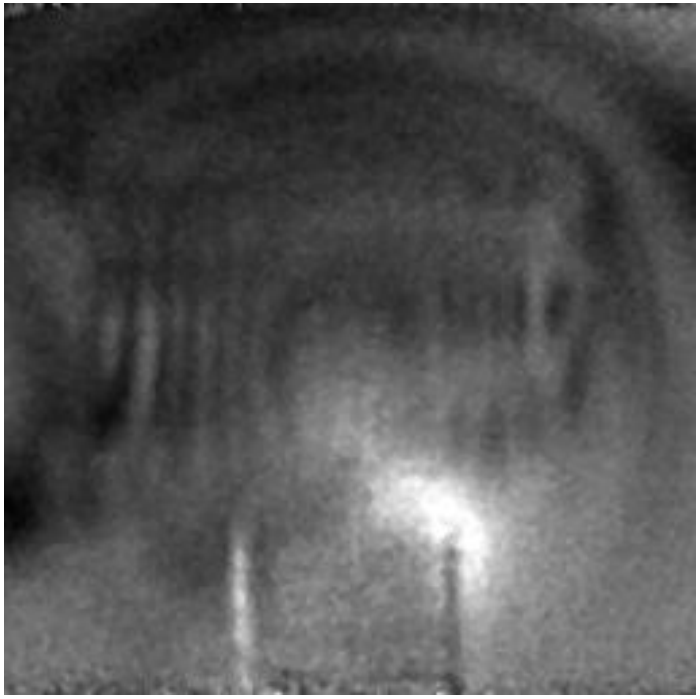

A. S. Tremsin, M. Dawson, N. Kardjilov, M. Strobl, I. Manke, J. B. McPhate, J. V. Vallerga, O. H. W. Siegmund, W. B. Feller, in preparation

Summary

- New neutron sensitive microchannel plates with very high detection efficiency of up to 70% for cold neutrons was produced and calibrated
- The spatial and timing resolution of those MCPs are as high as in previous generation (should be <15 μm and ~1 μs, respectively)
- High resolution neutron tomography, strain mapping and magneitc field imaging with MCP-Medipix2 detector can be performed

We would like to thank Medipix collaboration for the readout electronics (NIKHEF) and data acquisition software (IEAP, Prague) allowing user plugins.

This work was supported in part by the U.S. Department of Energy under Grants No. DE-FG02-07ER86322, DE-FG02-08ER86353 and National Science Foundation Grant No. DMR-0753599.

Neutron counting MCP detector with Medipix readout

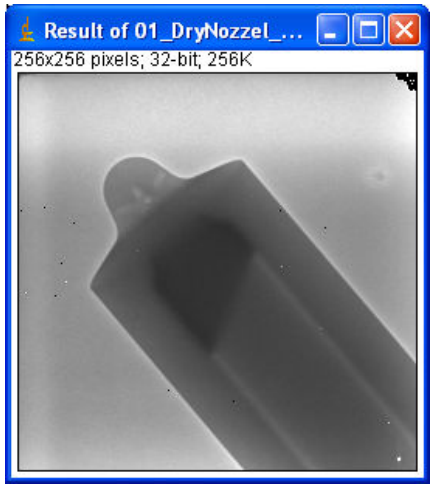

Fuel injection nozzle

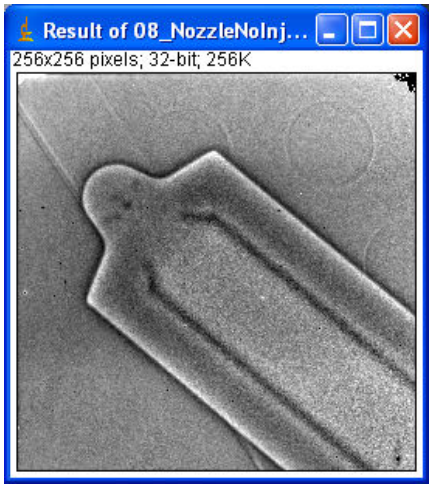

Dual energy image acquisition

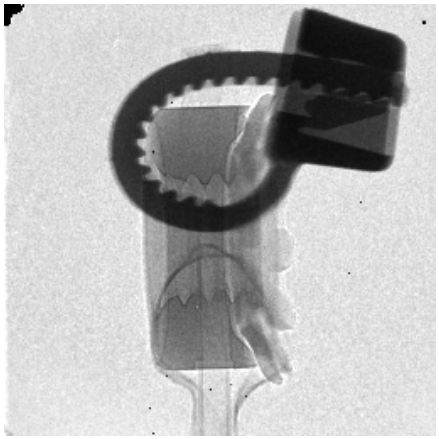

In collaboration with M. Muehlbauer, B. Schillinger, January 2009, FRM2, ANTARES beamline

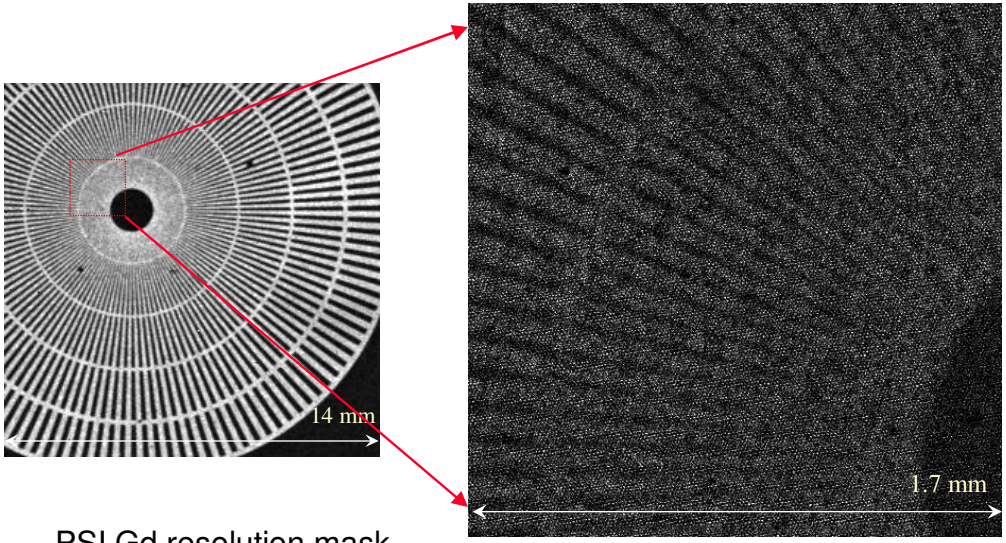

PSI Gd resolution mask

11 μm MCP pores are seen
Presently very low counting rate